

Chapter 6 Fluid Phase Equilibria of Ternary Mixtures

The fluid phase behaviour of many two-component mixtures has been comprehensively studied (Schneider, 1978 & 1991; Brunner, 1988 & 1990) over a wide range of both pressure and temperature. In contrast, the experimental study of three- or more-component mixtures is typically limited to isothermal and isobaric measurements either at, or near atmospheric conditions. This absence of data can be partly attributed to the great increase in resources that are required to comprehensively investigate multicomponent phase equilibria. Consequently, the basis of our knowledge of multicomponent mixtures is largely confined to observations of two-component phase equilibria typically involving only two phases. It is in this context that the calculation of critical properties has a valuable role in elucidating multicomponent phase equilibria. A critical transition occurs when all of the physical properties of coexisting phases become identical. The nature of the critical transition is a good indicator of the global nature of the phase behaviour of the fluid, as exemplified for binary fluid mixtures, by the work of van Konynenburg and Scott (1980) which is discussed in Chapter 5.

The phase behaviour of binary mixtures provides a useful but limited insight into the nature of the phase behaviour of multicomponent fluid mixtures in general. It is probable that phenomena exhibited by ternary mixtures are more representative of multicomponent fluid-phase equilibria than binary fluid behaviour. Although the complete experimental characterisation of a ternary mixture is a daunting undertaking, comprehensive calculations of the ternary critical surface are feasible. These calculations can be of value in elucidating the different types of phase equilibria exhibited by ternary mixtures, thereby, providing a window on the phase behaviour of multicomponent fluids.

6.1 Phase Behaviour of Ternary and Multicomponent Mixtures

In general, it is often assumed that the phase behaviour of ternary and multicomponent systems will be a relatively straightforward extension of the equilibria of binary mixtures. This view is probably justified if the component binary mixtures are completely miscible in all proportions. From the perspective of practical applications, this would constitute a very rare and fortuitous occurrence. In reality, the phase

behaviour of most ternary and other multicomponent systems is unlikely to be so simple. Ternary mixtures are likely to exhibit some phase transitions which are without counterpart in binary fluids. The phase behaviour of binary mixtures is distinguished from pure component equilibria by the effect of unlike interactions. By contrast, equilibria in ternary mixtures are influenced by different competing unlike interactions.

A considerable diversity of critical equilibria can be potentially observed in ternary mixtures. Sadus (1992, 1993) has reported the following types of critical transitions based on a phenomenological interpretation of critical calculations.

- (a) Class 1: Multiphase critical points (i.e., tricritical, tetracritical etc.) involving three or more phases undergoing a simultaneous transition to produce a single homogeneous phase. In the case of a tricritical point, the two menisci signifying the phase boundaries disappear simultaneously.
- (b) Class 2: Lower critical solution phenomena (LCST) and gas-liquid critical transition meet at a relatively low temperature. A critical transition occurs transforming the two-phase liquid-liquid equilibrium into a two-phase gas-liquid equilibrium. That is, the meniscus between the two liquid phases becomes critical simultaneously with the formation of a gas-liquid meniscus.
- (c) Class 3a: A region of lower critical solution temperature (LCST) and upper critical solution temperature (UCST) meet. The resulting critical transition is between the different two-phase liquid-liquid equilibria. That is, the lower solution meniscus disappears with the simultaneous formation of an upper critical solution meniscus.
- (d) Class 3b: There is a transition between two different two-phase upper critical solution menisci.

In this chapter, we will discuss the phase behaviour of two ternary systems: carbon dioxide + ethylene + helium and water + benzene + carbon dioxide ternary mixtures. For the carbon dioxide + ethylene + helium ternary mixture, we will present the predicted critical transitions results in comparison with experimental data. For water + benzene + carbon dioxide ternary mixture, we will show the prediction of the phase equilibria properties. In the last section, we will present some results from a theoretical study of ternary mixtures of equal size components.

6.2 Critical Transitions of the Carbon Dioxide + Ethylene + Helium Ternary Mixture

Experimental data for the critical transitions of ternary mixtures are extremely rare and typically confined to the vapour-liquid critical transition. A compilation of the gas-liquid critical transitions of approximately 60 ternary mixtures measured between the years 1945 and 1991 is available (Sadus, 1992a). The data of Tsiklis et al. (1970) for the carbon dioxide + ethylene + helium mixture are of particular interest. They reported critical transitions of this ternary system over a significant range of composition, temperature and pressure. The objective of the work in this part is to determine the critical surface for carbon dioxide + ethylene + helium and to compare the calculations with the available experimental data in order to verify both the accuracy of theory and, where possible, the existence of some of the above postulated critical transitions. The Guggenheim (1965) and Heilig-Franck (1989) equations of state are used in this work.

A feature of our calculation of ternary-mixture critical properties is that the required experimental inputs are limited to the critical properties of the individual component fluids and the binary interaction parameters (\mathbf{x}_{ij} and \mathbf{z}_{ij}) obtained from the analysis of the three binary sub-systems. In this case, we must first consider the phase behaviour of the binary carbon dioxide + ethylene, helium + carbon dioxide and helium + ethylene sub-systems.

The phase behaviour of carbon dioxide + ethylene is relatively straightforward. Rowlinson et al. (1958) reported a continuous critical curve linking the critical points of carbon dioxide and ethylene corresponding to Type I behaviour in the van Konynenburg and Scott (1980) classification scheme. In contrast, binary mixtures containing helium (Temkin, 1969) typically exhibit so-called "gas-gas" immiscibility of the first kind (Schneider, 1978, McGlashan, 1985, Rowlinson and Swinton, 1982). The critical locus commencing from the critical point of the component with the highest critical temperature extends directly to still higher temperatures and pressures without first passing through a temperature minimum. The phenomenon of "gas-gas" immiscibility of the first kind has been reported for both the helium + ethylene (Tsiklis, 1953) and helium + carbon dioxide (Tsiklis, 1952) systems to the extraordinary pressure of 800 MPa.

The comparison of theory with experiment for the three binary sub-systems is illustrated in Fig. 6.1 and the resulting interaction parameters are summarised in Table 6.1. The best fit values of ξ and ζ were obtained by repeatedly calculating the critical locus with different values of the adjustable parameters until optimal agreement was obtained with the experimental p - T data. Good agreement was also obtained for the p - x and T - x behaviour of the carbon dioxide + ethylene mixture. It is probable, judging by previous work (Sadus, 1994) that the p - x and T - x behaviour of the remaining binary sub-systems is also predicted with a reasonable degree of accuracy. However, there is insufficient experimental data to confirm this and it is likely that the predictions at very high pressure are less reliable than results obtained at low to moderate pressures. The Guggenheim (1965) and Heilig-Franck (1989) equations of state are of equal accuracy for the critical locus of the carbon dioxide + ethylene mixture. Similarly, calculations by means of these equations of state for both the helium + carbon dioxide and helium + ethylene systems are also in good agreement with experimental data. In view of the similar accuracy of both equations of state for the binary mixture properties, the simpler Guggenheim equation was adopted in preference to the Heilig-Franck equation for all subsequent ternary mixture calculations.

Table 6.1. Interaction parameters obtained from the analysis of binary mixtures using the Heilig-Franck and Guggenheim equations of state

| Binary Mixture | \mathbf{x}_{12} | | \mathbf{z}_{12} | |
|---|-------------------|------------|-------------------|------------|
| | Heilig-Franck | Guggenheim | Heilig-Franck | Guggenheim |
| He + CO ₂ | 1.850 | 1.685 | 1.015 | 1.012 |
| He + C ₂ H ₄ | 1.570 | 1.250 | 1.064 | 1.050 |
| CO ₂ + C ₂ H ₄ | 0.960 | 0.962 | 0.940 | 1.000 |

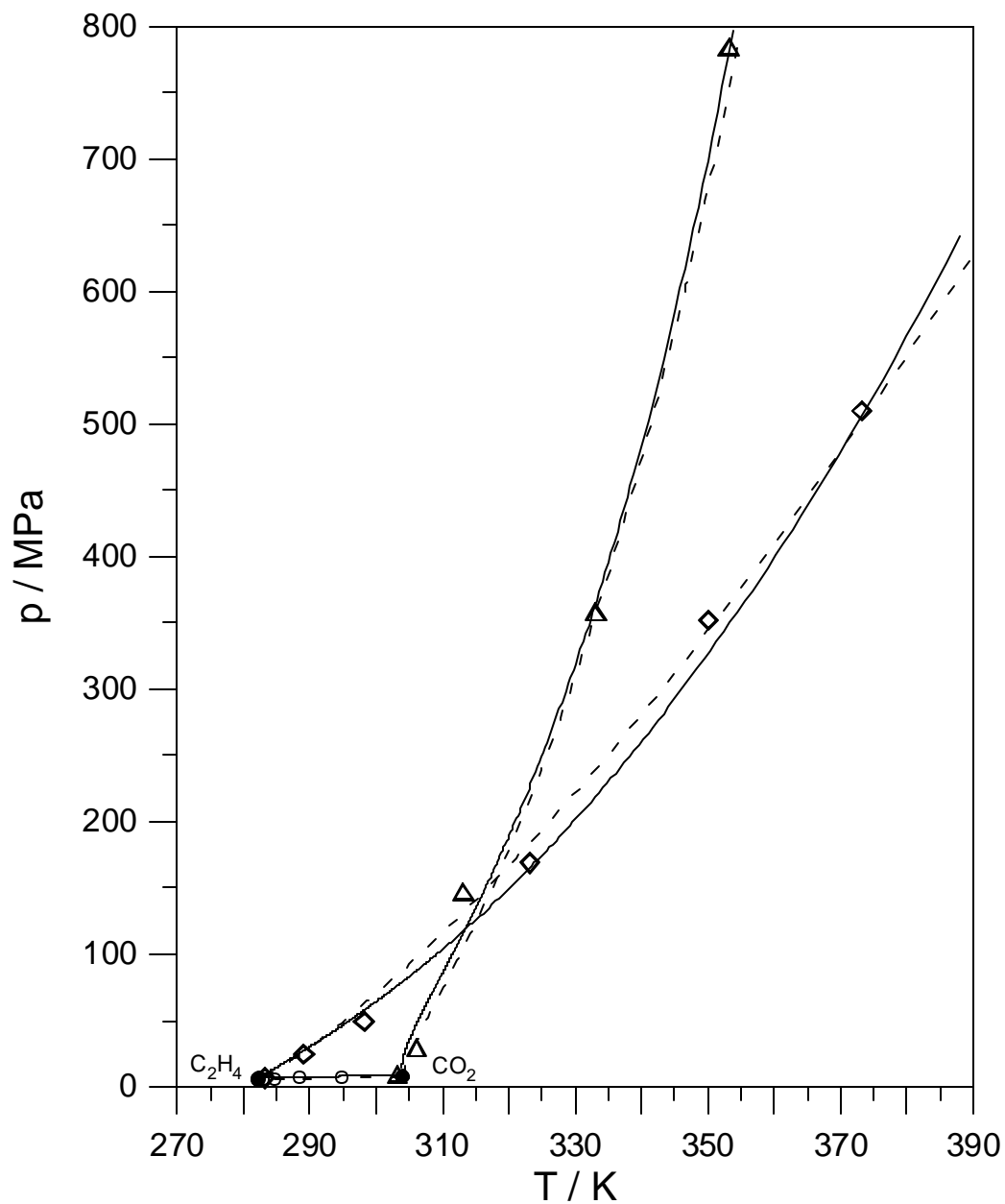


Fig. 6.1 Comparison of calculations using the Heilig-Franck (----) and Guggenheim (—) equations of state with experimental data for the binary mixtures carbon dioxide + ethylene (○; Rowlinson et al., 1958), helium + ethylene (◇; Tsiklis, 1953) and helium + carbon dioxide (△; Tsiklis, 1952) mixtures. The critical points (l) of carbon dioxide and ethylene are also illustrated.

Tsiklis et al. (1970) have reported experimental phase behaviour measurements and some critical transition data for the carbon dioxide + ethylene + helium ternary mixture. They reported a partial critical surface for the mixture and isothermal critical properties at 286.15, 293.15, 313.15, 333.15 and 343.15 K. The phase behaviour at 286.15 K is of particular interest. Below 20 MPa, only a single two-phase region stemming from the helium + carbon-dioxide binary mixture is apparent. So called "gas-gas" immiscibility in the helium + ethylene system commences at 20 MPa, and thereafter two distinct heterogenous regions are observed emanating from the helium + carbon dioxide and helium + ethylene binary sub-systems. At 30 MPa these two heterogeneous regions have a common critical point and a single, large two-phase region is created.

As we discussed in the previous chapters, the complete phase diagram of a binary mixture can be determined by solving the critical conditions for various increment of composition between a mole fraction of 0 and 1. However the additional dimension introduced by the third component in a ternary mixture generates a composition surface. This can be illustrated by the familiar equilateral triangle. Each apex represents one of the three pure components; the sides denote the constituent binary mixtures and the ternary mixture is represented by the interior space. More details are given by Sadus (1992a).

To obtain the critical surface of the carbon dioxide + ethylene + helium ternary mixture, several different *slices* were calculated corresponding to different fixed carbon dioxide/ethylene composition ratios. These varying cross-sectional profiles form the basis of the critical surface illustrated in Fig. 6.2. The ternary critical surface is bounded on three sides by the critical loci of the binary sub-systems. The region of "gas-gas" immiscibility evident in the helium + carbon dioxide and helium + ethylene binary mixtures is not as extensive in the ternary system. The addition of a third component increases the miscibility of the system. The shape of the ternary surface is akin to a billowing sail. Commencing from the carbon dioxide + ethylene critical locus, the ternary critical surface extends to initially lower temperatures, before passing through a temperature-pressure minimum and proceeding to higher temperatures and very high pressures. The calculated critical surface is consistent with the experimental data reported by Tsiklis et al. (1970).

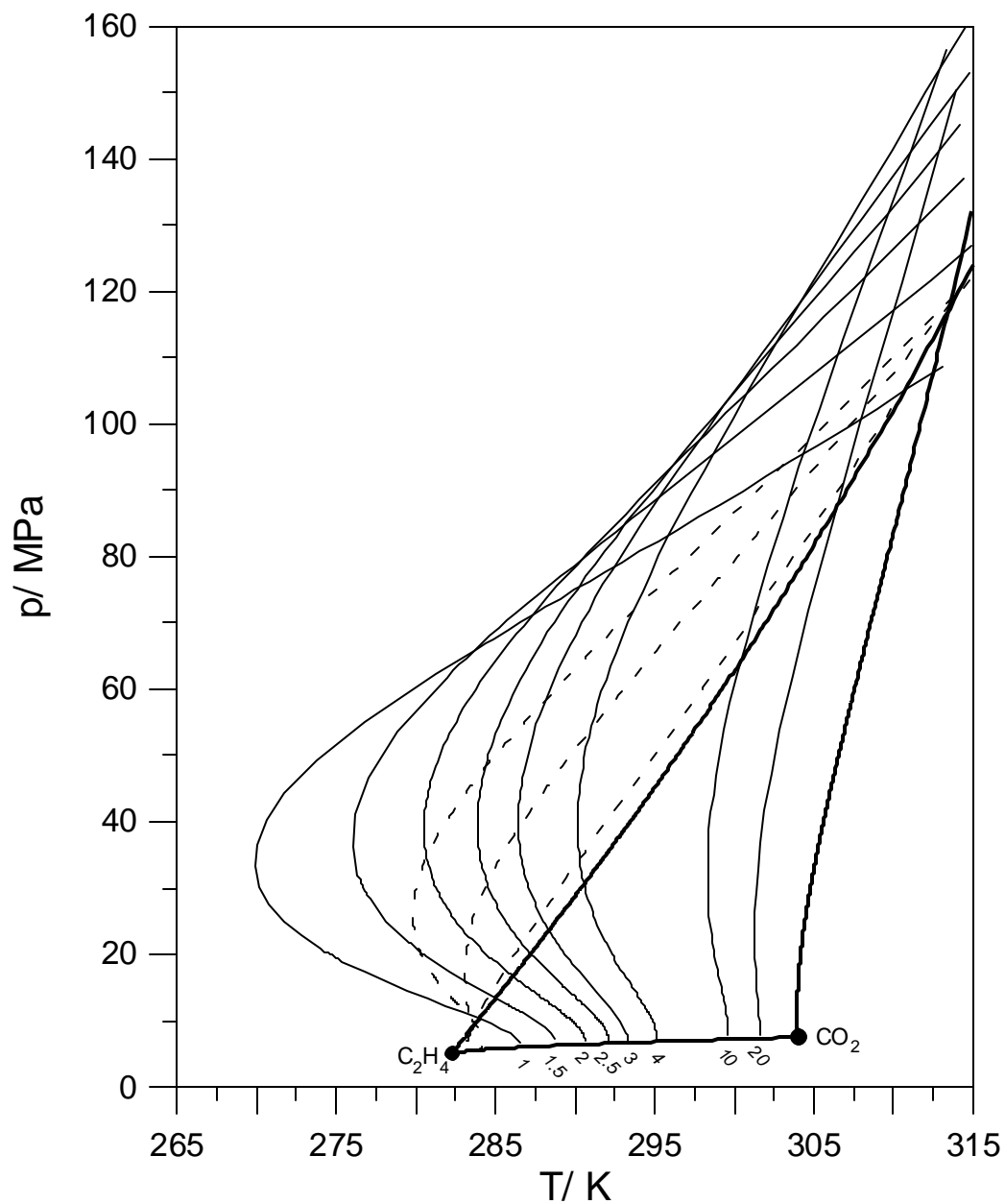


Fig. 6.2 The calculated critical surface of the carbon dioxide + ethylene + helium ternary mixture. The labels indicate the contribution from the various cross-sectional profiles at a constant carbon dioxide/ethylene ratio. Calculations for ratios < 1 are illustrated by the unlabelled broken lines. The critical properties of the binary subsystems (—) and the critical points (●) of ethylene and carbon dioxide are also illustrated.

A comparison of theory with the experimental data of Tsiklis et al. for the critical isothermal-composition behaviour of the ternary mixture is illustrated in Fig. 6.3. The ternary calculations are genuine a priori predictions without any reliance on experimental ternary data. It should be noted that Tsiklis et al. (1970) directly measured the critical temperature and pressure but they only estimated the critical composition. A "double critical point" was reported at 286.15 K. The calculations confirm the existence of such a transition at this temperature but there is a disparity in the corresponding critical pressure and composition (the predicted coordinates are: $x_{C_2H_4} = 0.158$, $x_{CO_2} = 0.474$, $x_{He} = 0.368$, $V^c = 54.10 \text{ cm}^3 \cdot \text{mol}^{-1}$, $p^c = 40.54 \text{ MPa}$). It is apparent from Fig. 6.3 that theory and experiment at 286.15 K are only in qualitative agreement. The predicted one-phase region is substantially greater than that observed experimentally. The calculations are also in qualitative agreement with experiment at 293.15, 313.15, 333.15 and 343.15 K but the discrepancy between theory and experiment is less serious. At 313.15 K and 333.15 K, the accuracy of the ternary analysis is hampered by the inaccuracy of the calculated critical composition for the binary mixtures.

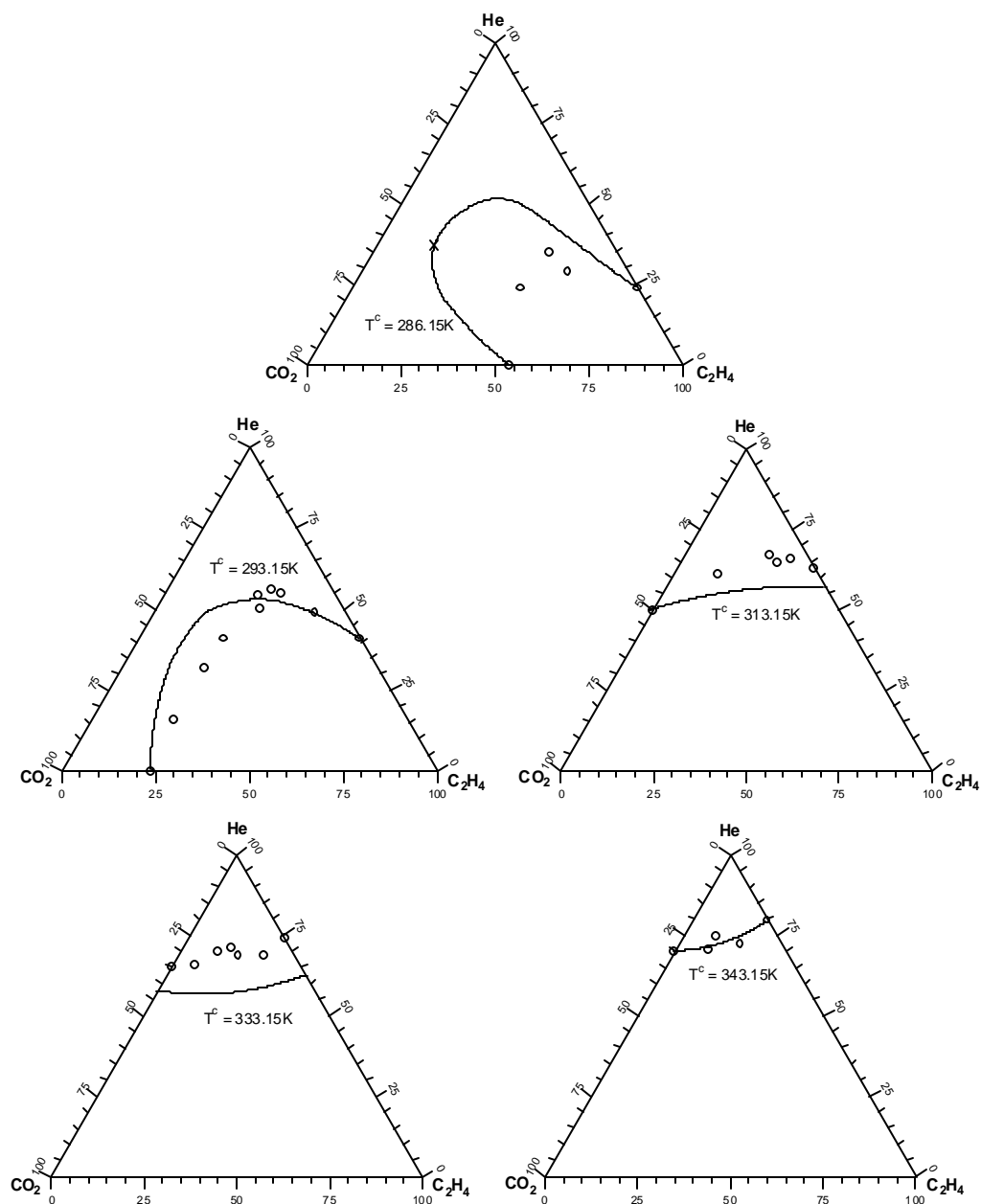


Fig. 6.3 Comparison of calculations (—) with the experimental data of Tsiklis et al. (O; Tsiklis et al., 1970) for the isothermal-composition behaviour of the ternary mixture carbon dioxide + ethylene + helium at various temperatures. The position of a double critical point at 286.15 K is indicated (x).

6.3 Phase Behaviour of the Water + Benzene + Carbon Dioxide Ternary Mixture

Brandt (1987) reported experimental phase equilibria curves of ternary mixture water + benzene + carbon dioxide over a large range of pressure and temperature. In this part, we will predict the phase equilibria curves of this ternary mixture and discuss the results. The Guggenheim and Heilig-Franck equations of state are used.

6.3.1 Critical Transition of the Water + Benzene + Carbon Dioxide Ternary Mixture

As we discussed in 6.2, before the phase behaviour of the water + benzene + carbon dioxide ternary mixture can be calculated, the phase behaviour of the binary mixtures water + benzene, water + carbon dioxide and benzene + carbon dioxide sub-systems must be considered. Hicks and Young (1975) listed the experimental data for these three binary mixtures. The phase behaviour of benzene + carbon dioxide corresponds to Type I behaviour in the van Konynenburg and Scott (see Chapter 5) classification scheme because it has a continuous critical curve linking the critical points of two components: benzene and carbon dioxide. For the phase behaviour of binary mixtures containing water, Type III behaviour is showed. For the water + benzene binary mixture, the critical curve starts from the critical point of water, passes through a temperature minimum and rapidly goes to high pressure. This phenomenon corresponds to so-called "gas-gas" immiscibility of the second kind (Schneider, 1978, McGlashan, 1985, Swinton, 1982). For water + carbon dioxide, the critical curve also starts from the critical point of water, passes through a temperature minimum (Tödheide and Franck (1963) reported at 539 K and 245 MPa) and moves to very high pressure. The comparison of theory with experiment made by using the Guggenheim and Heilig-Franck equations of state for these three binary sub-systems is presented in Fig. 6.4 and the resulting interaction parameters are summarised in Table 6.2. It is apparent from Fig. 6.4 that the critical curves predicted by these two equations of state are in good agreement with experimental data.

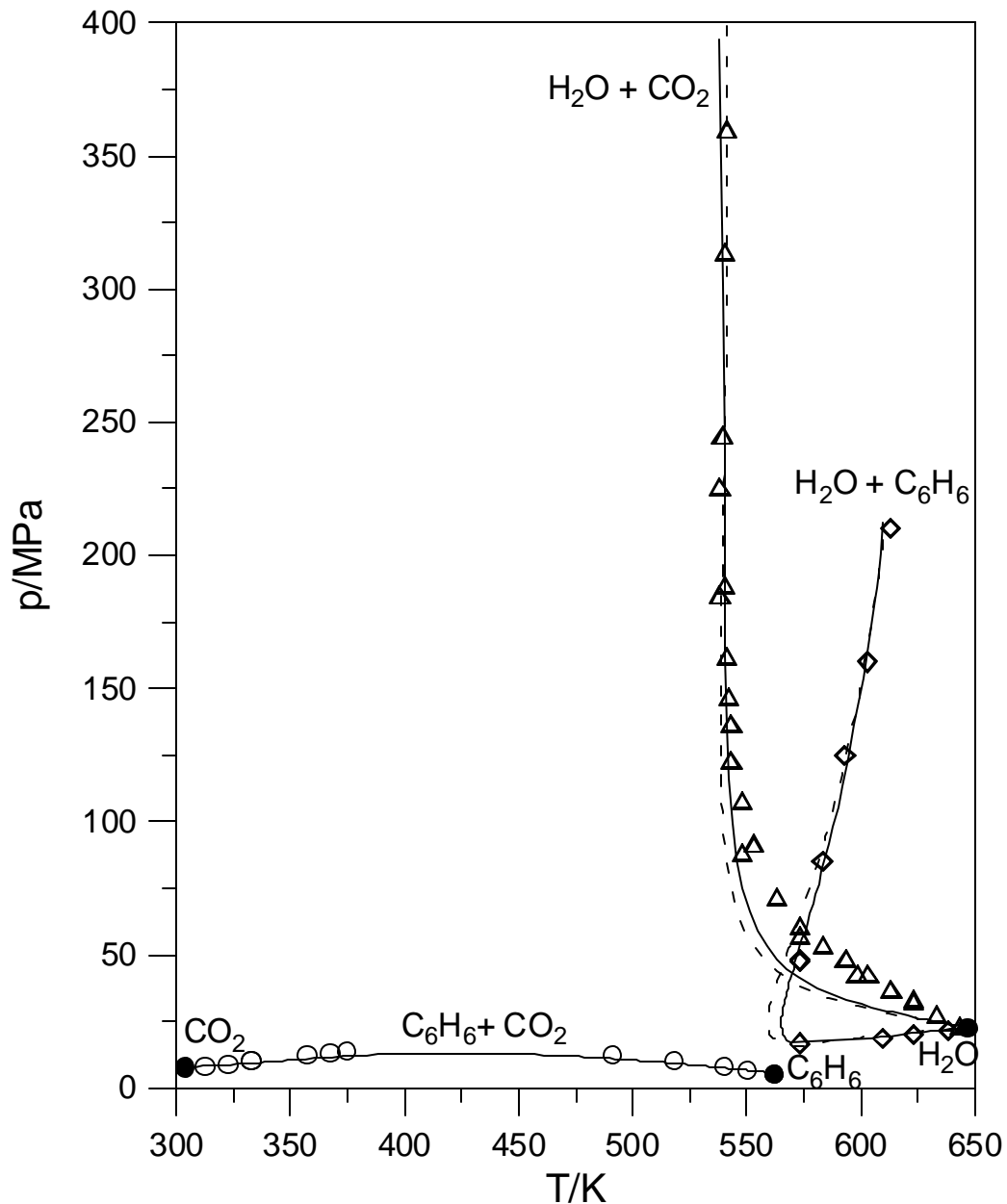


Figure 6.4 Comparison of calculations using the Heilig-Frank (—) and Guggenheim (---) equations of state with experimental data for the binary mixtures water + carbon dioxide (Δ) (Hicks and Young, 1975), water + benzene (\diamond) (Hicks and Young, 1975) and benzene + carbon dioxide (\circ) (Hicks and Young, 1975; Kay and Kreglewski, 1983). The critical points (l) of water, benzene and carbon dioxide are also illustrated.

Table 6.2. Interaction parameters obtained from the analysis of binary mixtures using the Heilig-Franck and Guggenheim equations of state

| Binary Mixture | \mathbf{x}_{12} | | \mathbf{z}_{12} | |
|--|-------------------|------------|-------------------|------------|
| | Heilig-Franck | Guggenheim | Heilig-Franck | Guggenheim |
| H ₂ O + CO ₂ | 0.802 | 0.795 | 0.925 | 0.940 |
| H ₂ O + C ₆ H ₆ | 0.772 | 0.750 | 0.940 | 0.940 |
| C ₆ H ₆ + CO ₂ | 0.800 | 0.800 | 1.000 | 1.000 |

Brandt (1987) reported experimental critical curves of the water + benzene + carbon dioxide ternary mixture at constant water, benzene or carbon dioxide ratio without tabulated experimental data. By using the same idea, we present the calculated critical curves of the water + benzene + carbon dioxide mixture at constant ratio of composition of water (Fig 6.5), benzene (Fig. 6.6) and carbon dioxide (Fig. 6.7). The Guggenheim equation of state is used in calculations. The labels, for example 20, 30, 40, 70, 93 etc, indicate the contribution from the various cross-sectional profiles at constant ratio of composition of water (Fig 6.5), benzene (Fig. 6.6) and carbon dioxide (Fig. 6.7). Overall these three diagrams, each diagram consists of two different parts of critical transition regardless fixed ratio of composition. The first part is in the region of higher temperature (greater than the critical temperature of pure component benzene and less than the critical temperature of water) and higher pressure (minimum pressure is about 15 MPa). The second part is in the range of lower temperature (less than the critical temperature of pure component benzene and greater than the critical temperature of carbon dioxide) and lower pressure (greater than the critical pressure of benzene and maximum pressure is about 15 MPa).

Because of the lack of experimental data, the calculated critical curves (Fig 6.5, 6.6 and 6.7) can only be compared with Brandt's (1987) graphical results (Fig. 56, Fig. 57, Fig. 58 in Brandt's (1987) thesis). Generally the agreement between calculation and Brandt's results is quantitatively good. However, it is noticeable that there is a difference for the critical curve at lower critical temperatures.

The critical transition of this ternary mixture is interesting. Fig 6.5, Fig 6.6 and Fig 6.7 show the calculated critical curves of the water + benzene + carbon dioxide ternary mixture at different ratios of composition of water (Fig 6.5), benzene (Fig. 6.6) and carbon dioxide (Fig 6.7). According to the behaviour of critical curves at different perspective, we can group all calculated critical transitions into liquid-liquid (lower pressure part) and vapour-liquid (higher pressure part) transitions. For example, when the ratio of composition of water is fixed, we can summarise the critical behaviour of this ternary mixture as follows:

- (a) Liquid-liquid transitions: when the fixed ratios are less than 70, the critical behaviour of ternary mixture behaves like liquid-liquid surfaces. The critical curves start at the side close to the critical point of benzene, extend to the lower temperatures and stop at end point curve. The tendency of these critical curves is similar with the critical curve of binary mixture benzene + carbon dioxide. When the fixed ratio of water is greater than 70 and less than about 81, there are two parts of critical curves. One part is liquid-liquid surfaces. Another part behaves vapour-liquid transition. When the fixed ratio of water is great than 80 and less than about 90, the liquid-liquid transition disappears as the ratio increases from 80.
- (b) Vapour-liquid transitions: this part starts from the critical curve of binary mixture water + carbon dioxide, moves to the lower temperature and goes rapidly to high pressure. When the fixed ratios are great than 80, the vapour-liquid curve begins from the critical curve of binary mixture water + carbon dioxide, goes to lower pressure and lower temperature, passes a minimum pressure and rises directly to very high pressure. The tendency of this critical behaviour is of the same as that of binary mixture water + benzene. As the fixed ratios increase from 90, the critical curves of this ternary mixture become simple. They start from the critical curve of binary mixture water + carbon dioxide and end at the critical curve of binary mixture water + benzene. Obviously, when the ratio closes to 100, the critical curve of this ternary mixture becomes one point, the critical point of water.

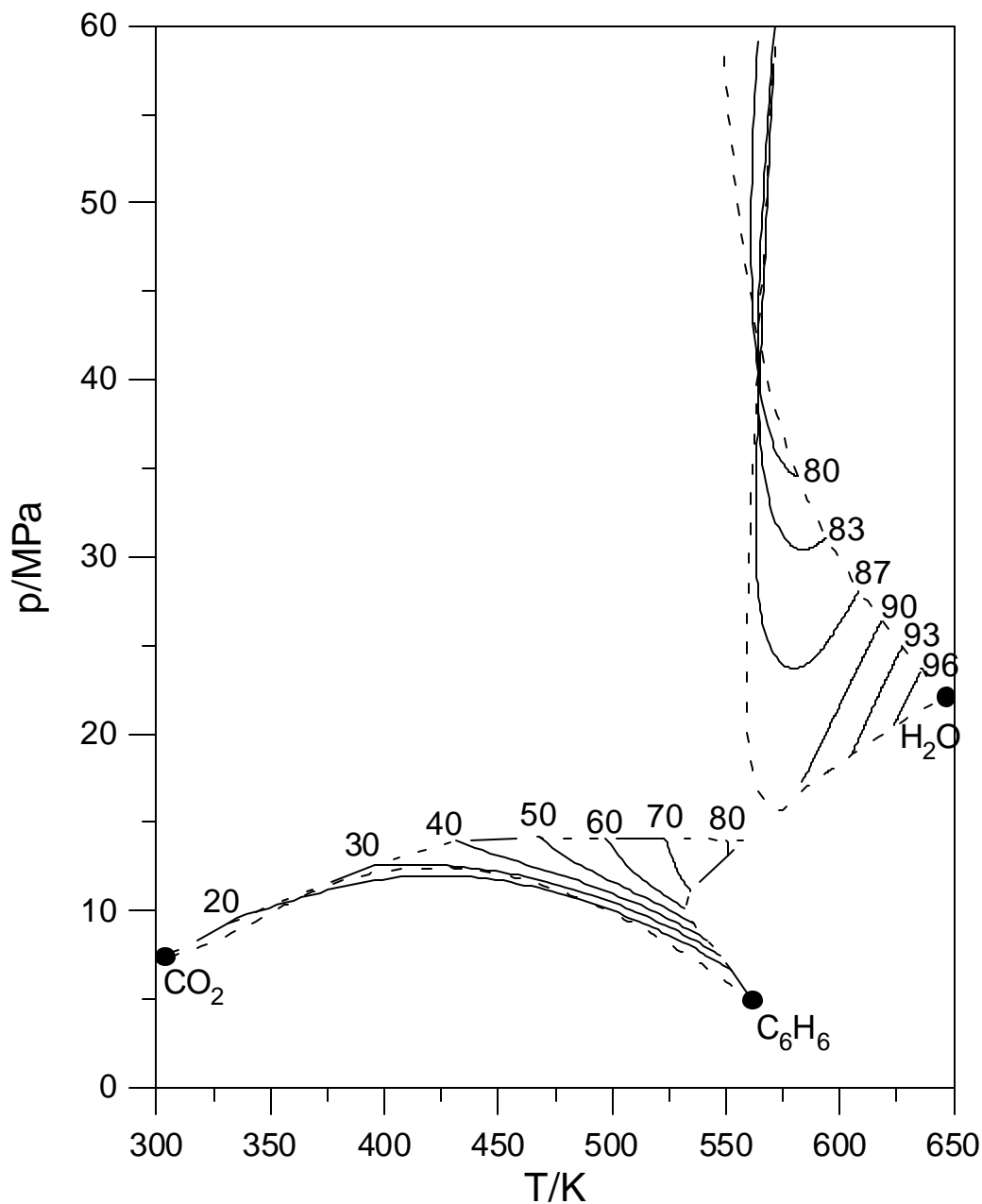


Fig. 6.5 The calculated critical curves (—) of the water + benzene + carbon dioxide ternary mixture. The labels indicate the contribution from the various cross-sectional profiles at a constant water ratio (H_2O fixed). The critical end-point curve (— ···), the critical properties of the binary sub-systems (— —) and the critical points (●) of water, benzene and carbon dioxide are also illustrated. Estimated curves can also be found in Fig. 57 of Brandt's (1987) thesis.

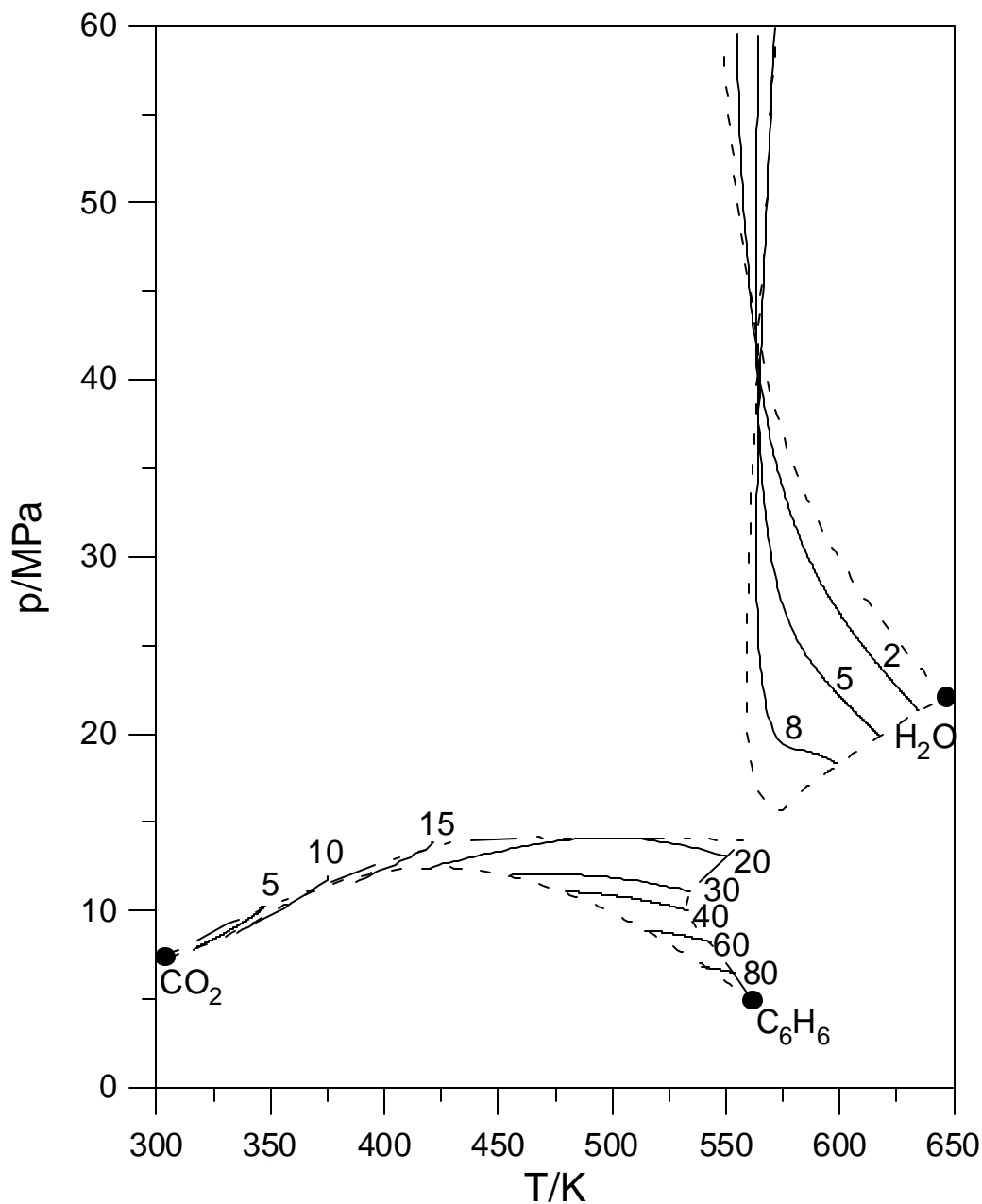


Fig. 6.6 The calculated critical curves (—) of the water + benzene + carbon dioxide ternary mixture. The labels indicate the contribution from the various cross-sectional profiles at a constant benzene ratio (C_6H_6 fixed). The critical end-point curve (— ···), the critical properties of the binary sub-systems (— — —) and the critical points (l) of water, benzene and carbon dioxide are also illustrated. Estimated curves can also be found in Fig. 56 of Brandt's (1987) thesis.

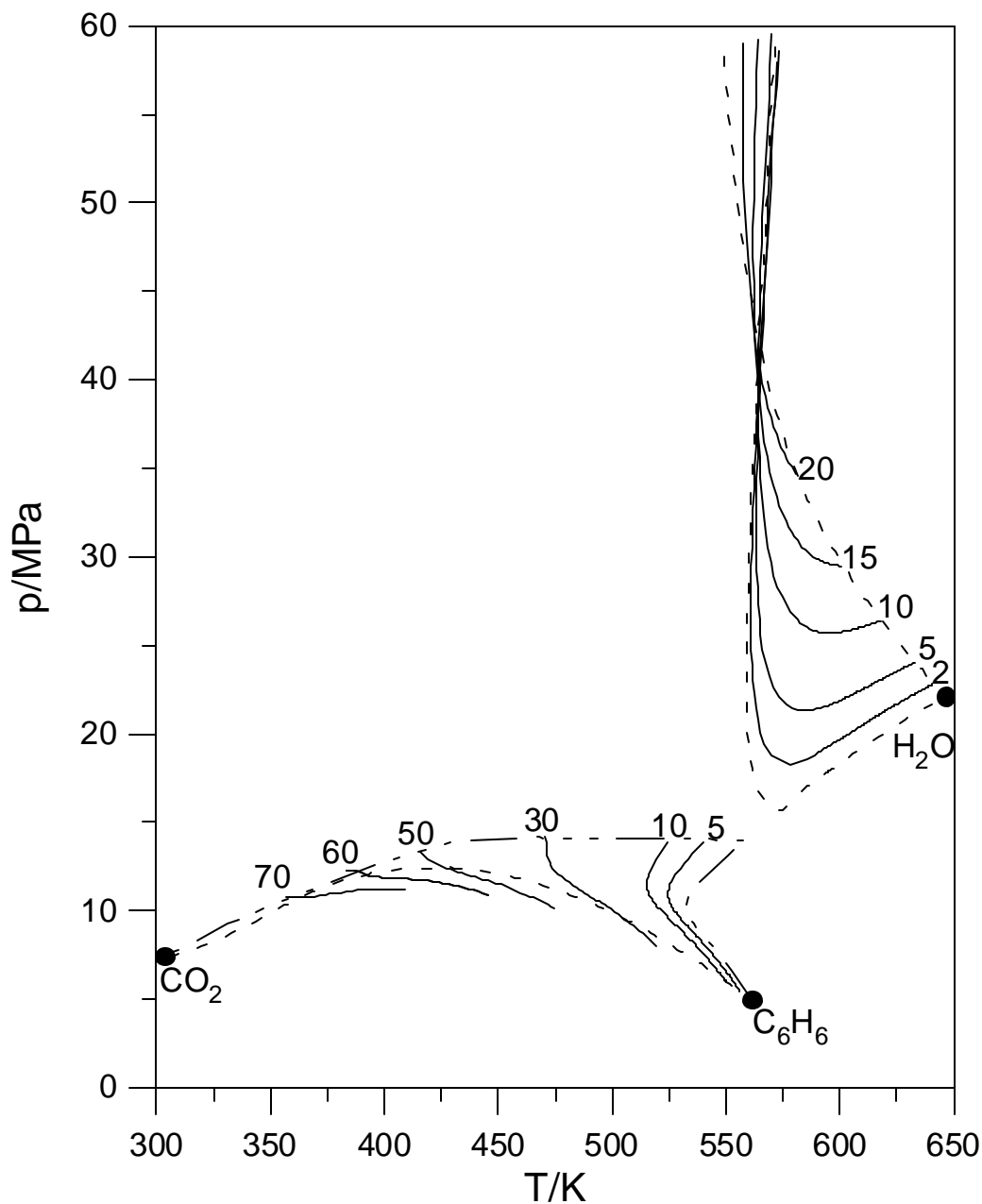


Fig. 6.7 The calculated critical curves (—) of the water + benzene + carbon dioxide ternary mixture. The labels indicate the contribution from the various cross-sectional profiles at a constant carbon dioxide ratio (CO_2 fixed). The critical end-point curve (— · · ·), the critical properties of the binary sub-systems (— — —) and the critical points (●) of water, benzene and carbon dioxide are also illustrated. Estimated curves can also be found in Fig. 58 of Brandt's (1987) thesis.

6.3.2 Phase Equilibria of the Water + Benzene + Carbon + Dioxide Ternary Mixture

Brandt (1987) reported experimental phase behaviour for water + benzene + carbon dioxide ternary mixture over a large range of temperature and pressure. However, much of the experimental data was not tabulated but only presented graphically. Therefore, we can only qualitatively compare our results with the experimental curves reported (Brandt, 1987). The adjustable binary parameters for the water + benzene, water + carbon dioxide and benzene + carbon dioxide (Table 6.2) were used without modifications to predict the phase behaviour of this ternary system.

The predicted ternary composition diagrams of this mixture at different temperatures and a fixed pressure of 22.1 MPa is shown in Fig. 6.8. The solid lines correspond to predictions made by the Guggenheim equation of state at different temperatures. The overall results show that the calculations are in qualitative agreement with experimental curves (Brandt, 1987) and the discrepancy between theory and experiment is less serious compared to Brandt's (1987) results. At $T = 323$ K, the phase equilibria line of the ternary mixture connects two phase equilibrium points of binary mixtures water + benzene and water + carbon dioxide. As temperature is increased, the tendency of the line is changed. Theoretically, the two curves could meet at a tricritical point at temperature between 555 K and 558 K and then separate to different directions. Finally, only one part is left which starts and ends at the binary mixture water + carbon dioxide. It is apparent from Fig. 6.8 that the calculation fails for some points, for example $T = 558$ K and $T = 563$ K. This may be because the compositions of two phases are very close to each other.

The predicted ternary composition diagrams of this ternary mixture at fixed pressures of 65 MPa, 108 MPa and 300 MPa and different temperatures are also shown in Fig. 6.9, Fig. 6.10 and Fig. 6.11, respectively. Apart from the common lower temperature behaviour (from $T = 323$ K to $T = 523$ K for Fig. 6.9), the behaviour at $T = 537.47$ K and $T = 537.49$ K in Fig. 6.9 is of interest. At $T = 537.47$ K, both liquid-liquid equilibria lines, which both connect the binary mixtures water + benzene and water + carbon dioxide, approach each other but they do not meet and suddenly change to different directions. However, at $T = 537.49$ K, these two lines meet at a possible tricritical point of the ternary mixture. As the temperature is increased, the tendency of these two lines change their direction. In contrast to Fig 6.8 ($p = 22.1$ MPa), the part which starts and ends at the binary mixture water + carbon dioxide disappears first and

only the part which starts and ends at the binary mixture water + benzene exists. Since the composition of two phases are not very close to each other, the complete calculations are fully implemented for $p = 65$ MPa. Comparison with Brandt's (1987) graphical experimental results, the calculations are in qualitative agreement with experiment and the discrepancy between theory and experiment is less serious. For example, at $p = 65$ MPa two phase equilibria curves meet at $T = 543$ K from experimental results, the calculation (Fig. 6.9) shows that they meet at 537.49 K. Similar results have obtained for $p = 108$ MPa (Fig. 6.10) and $p = 300$ MPa (Fig. 6.11) but no experimental meeting points were reported for these two pressures.

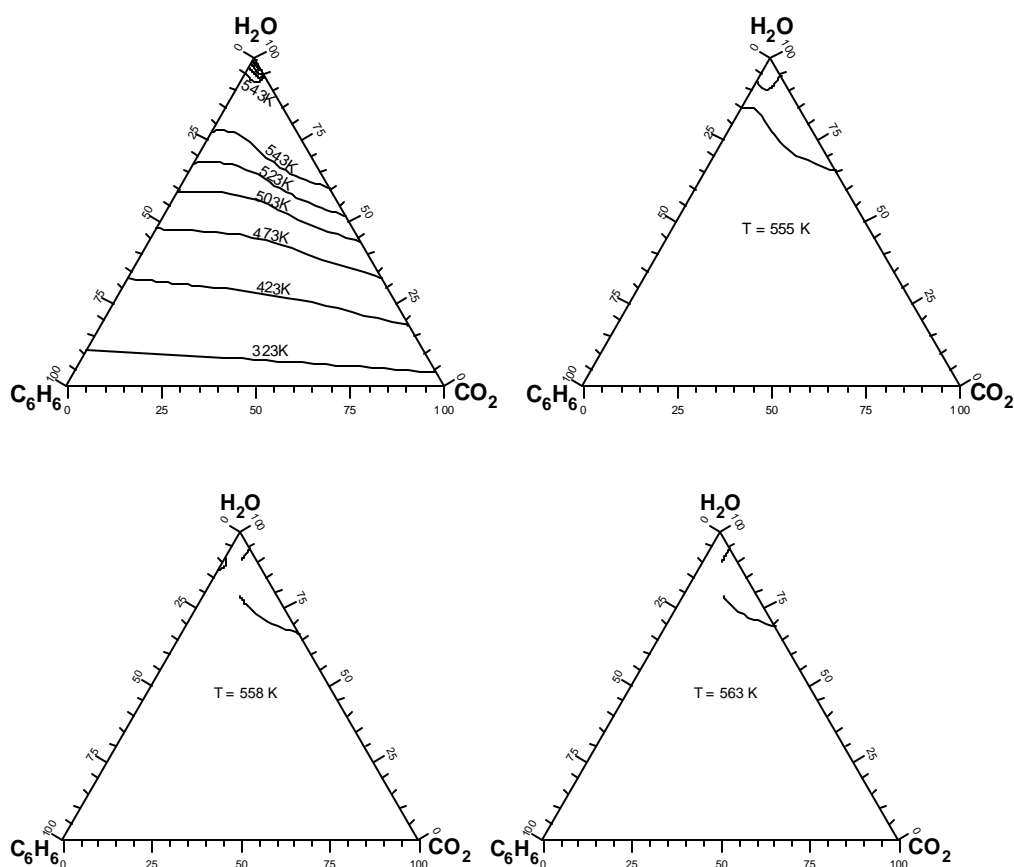


Figure 6.8 Predicted ternary diagrams for water + benzene + carbon dioxide at $p = 22.1$ MPa and various temperatures.

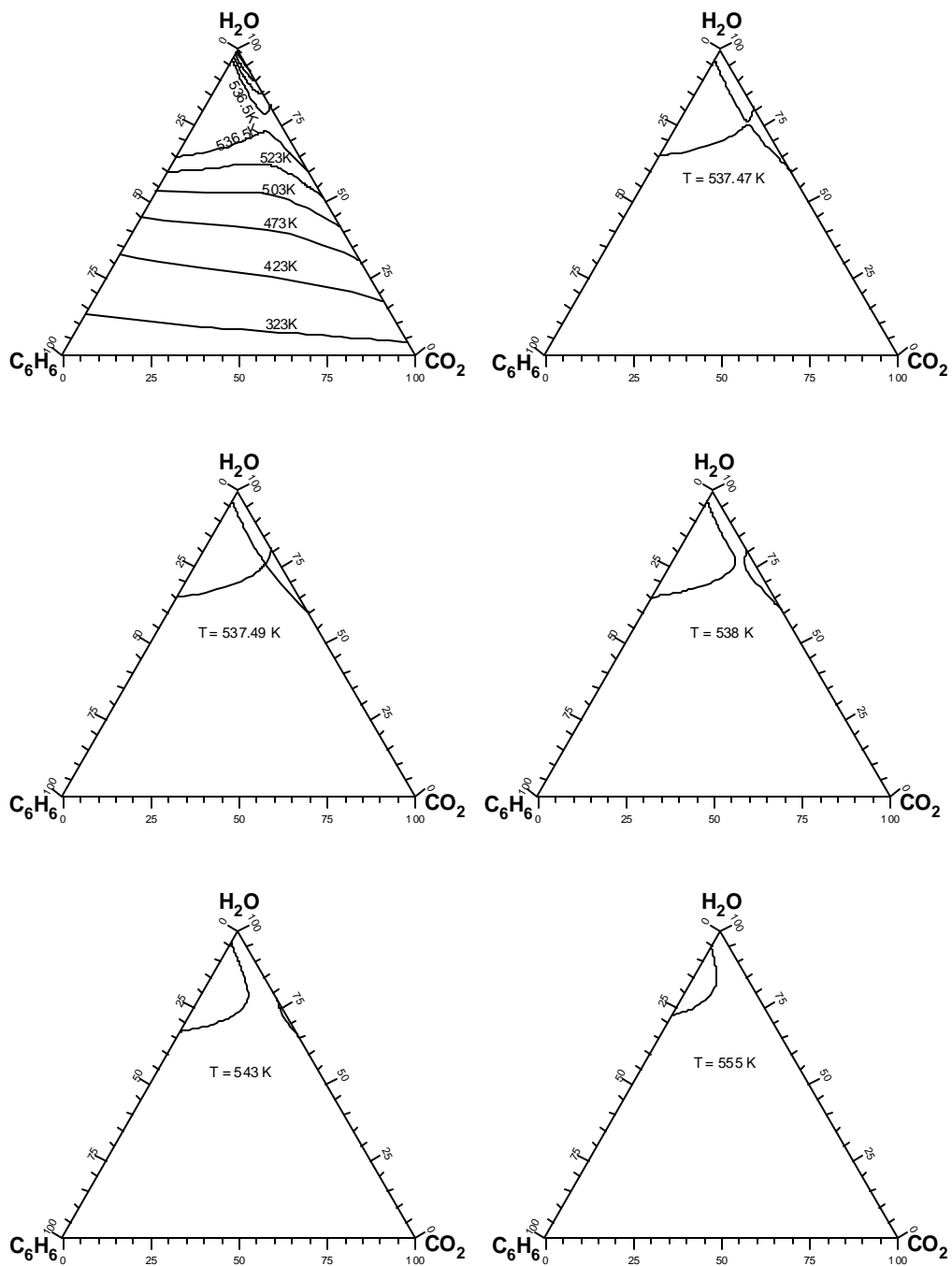


Figure 6.9 Predicted ternary diagrams for water + benzene + carbon dioxide at $p = 65$ MPa and various temperatures.

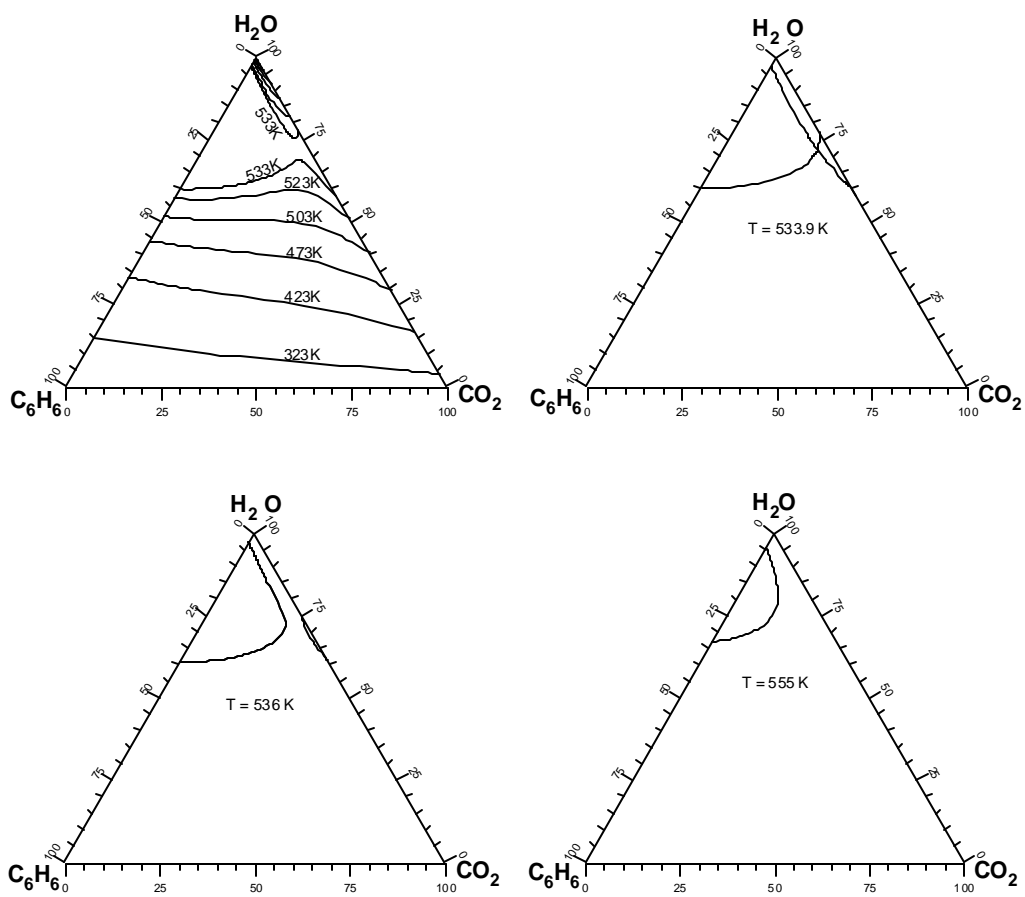


Figure 6.10 Predicted ternary diagrams for water + benzene + carbon dioxide at $p = 108\text{ MPa}$ and various temperatures.

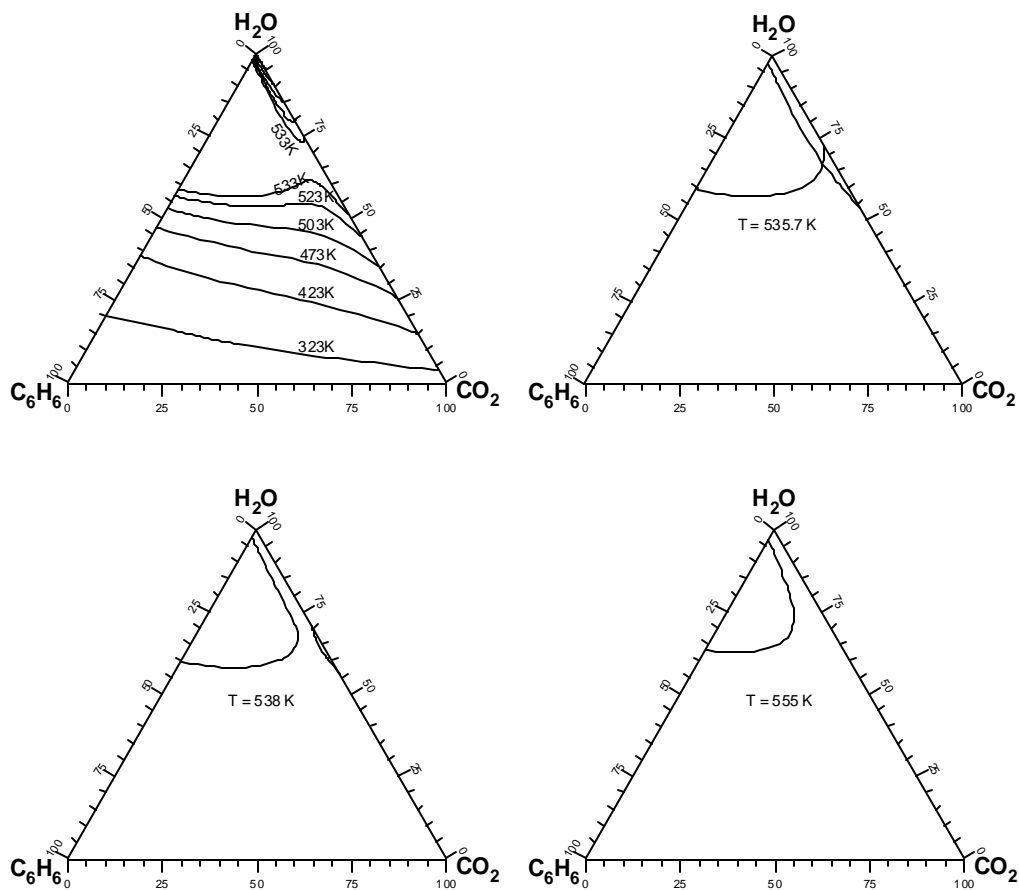


Figure 6.11 Predicted ternary diagrams for water + benzene + carbon dioxide at $p = 300 \text{ MPa}$ and various temperatures.

6.4 Theoretical Study of Ternary Mixtures of Equal Size Components

The phase behaviour of binary mixtures depends on the relative size of the conformational parameters (h and f) between the component molecules. The theory of conformational solutions was discussed in Chapter 2. Mixtures with components with identical or similar conformational parameters exhibit Type I behaviour whereas liquid-liquid phenomenon is observed when there is a substantial difference in the conformational parameters. Generally, the f conformational parameter plays the dominant role in determining the phase behaviour.

The link between the conformational parameters and the phase behaviour type allows us to construct ternary mixtures of different binary phase behaviour types governed solely by the ratio of the conformational parameters and assuming the following combining rules for the unlike interaction (see Chapter 3)

$$f_{12} = \sqrt{f_{11}f_{22}} \quad (6.1)$$

The complexity of the binary mixtures can be simplified by using molecules of equal size. For the equal size case, $h_{11} = h_{22} = h_{12} = 1$ and the properties of mixture are determined solely by the f conformational parameter.

The first step in the analysis is to determine the values of f_{11} and f_{22} which will result in the different types of phase behaviour. Calculations were performed with Guggenheim equation of state at different values of f_{11} and f_{22} . The results are summarised in Table 6.3.

Table 6.3 The parameters of binary mixtures

| Mixture | Phase behaviour Type | f_{11} | f_{22} |
|---------|-------------------------|----------|----------|
| A | I | 0.95 | 1.0 |
| B | I | 0.85 | 1.0 |
| C | I | 0.65 | 1.0 |
| D | I | 1.0 | 0.85 |
| E | I | 0.65 | 0.85 |
| F | I | 0.85 | 0.49 |
| G | I | 0.5 | 0.485 |
| H | I | 0.65 | 0.43 |
| I | I | 0.5 | 0.43 |
| J | I | 0.45 | 0.25 |
| K | II | 0.485 | 1.0 |
| L | II | 0.5 | 1.0 |
| M | II | 1.0 | 0.485 |
| N | II | 1.0 | 0.49 |
| O | II | 1.0 | 0.5 |
| P | II | 0.95 | 0.485 |
| Q | II | 0.85 | 0.43 |
| R | II | 0.5 | 0.25 |
| S | II | 0.45 | 0.22 |
| T | III | 0.45 | 1.0 |
| U | III | 1.0 | 0.43 |
| V | III | 1.0 | 0.25 |
| W | III | 1.0 | 0.22 |
| X | III | 0.95 | 0.43 |
| Y | III | 0.5 | 0.22 |

Table 6.4 Possible combinations of binary mixture types in a ternary mixture *

| 1st Sub binary mixture | 2nd Sub binary mixture | 3rd Sub binary mixture | Is the combination of binary mixtures possible? |
|------------------------|------------------------|------------------------|---|
| C (I) | D (I) | E (I) | Yes |
| I | I | II | No |
| I | I | III | No |
| B (I) | N (II) | F (I) | Yes |
| A (I) | M (II) | P (II) | Yes (Ternary mixture 1) |
| I | II | III | No |
| C (I) | U (III) | H (I) | Yes |
| B (I) | U (III) | Q (II) | Yes |
| A (I) | U (III) | X (III) | Yes (Ternary mixture 2) |
| K (II) | O (II) | G (I) | Yes |
| II | II | II | No |
| II | II | III | No |
| L (II) | U (III) | I (I) | Yes |
| L (II) | V (III) | R (II) | Yes |
| L (II) | W (III) | Y (III) | Yes (Ternary mixture 3) |
| T (III) | V (III) | J (I) | Yes |
| T (III) | W (III) | S (II) | Yes |
| III | III | III | No |

* The phase type of the sub binary mixture is given in brackets

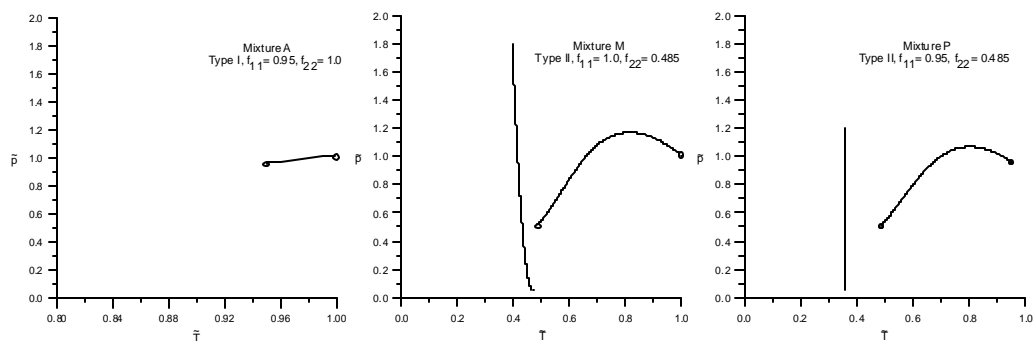
Only Type I, II and III phase behaviour types could be generated by varying the f parameter. To obtain the same type or different type of critical behaviour of binary mixture, different f_{11} or f_{22} can be used (Table 6.3). For example, to obtain Type III behaviour, $f_{22} = 0.43$ is used for binary mixture U whereas $f_{22} = 0.22$ is used for binary mixture W although both binary mixture U and W are of Type III behaviour.

From Type I, II and II phase behaviour of binary mixtures, 18 possible combinations of the ternary mixtures could be formed and these combinations listed in Table 6.4. The first column in Table 6.4 is the first sub binary mixture for which the critical curve is obtained by using varying f_{11} only ($f_{22} = 1.0$). The second column is

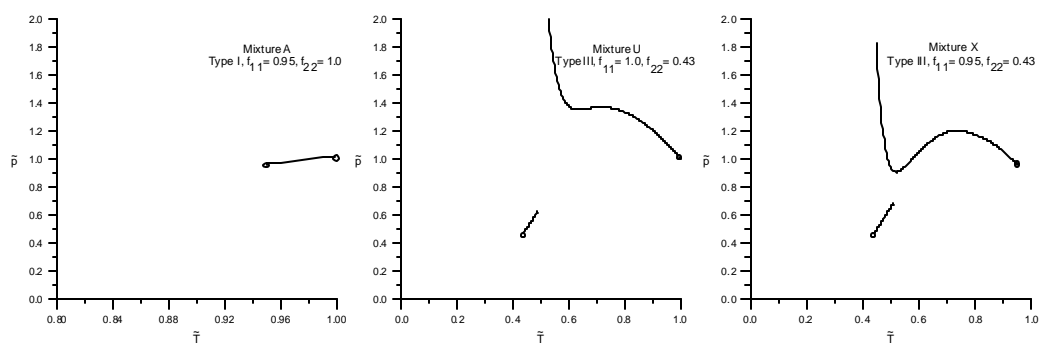
the second sub binary mixture for which the critical curve is obtained by varying f_{22} only ($f_{11}=1.0$). The third column is the third sub binary mixture for which the critical curve is obtained by using f_{11} and f_{22} which directly come from the first and the second sub binary mixtures. For example, for the ternary mixture 1 (Table 6.4), the first sub binary mixture is binary mixture A with $f_{11}=0.95$ and $f_{22}=1.0$ and the second sub binary mixture is binary mixture M with $f_{11}=1.0$ and $f_{22}=0.485$. Therefore, the f parameters of the third sub binary mixture directly come from the first and the second sub binary mixture. That is why we used $f_{11}=0.95$ and $f_{22}=0.485$ for Mixture P. Because the parameter f_{11} of the first sub binary mixture and f_{22} of the second sub binary mixture were used to form the third sub binary mixture, the third binary mixture is not always possible. In other words, a related ternary mixture is not always possible. Our calculations show only 12 combinations result in a viable third sub binary mixtures. The possibility of the combination of third sub binary mixtures is indicated by the fourth column in Table 6.4, "Yes" means that the type of third sub binary mixture can be obtained by using the same f_{11} and f_{22} which come from the first and the second sub binary mixtures.

It is hard to present all details for 12 possible ternary mixtures. In this section, we report three of twelve ternary mixtures, mixture 1, mixture 2 and mixture 3. They are also identified in Table 6.4. As we mentioned in 6.2, before the phase behaviour of ternary mixture 1, mixture 2 and mixture 3 can be calculated, the phase behaviour of the sub binary mixtures must be considered.

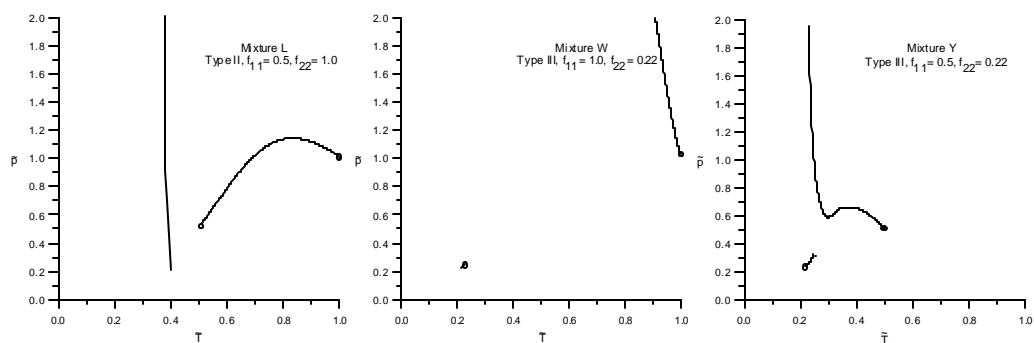
The critical curves of sub binary mixtures (mixture A, M, P, U, X, L, W, Y) in p - T (reduced pressure $\tilde{p} = p/p_{00}^C$ and reduced temperature $\tilde{T} = T/T_{00}^C$) projection are given in Fig. 6.12. It is noticeable from Fig. 6.12 that the scale of temperature of binary mixture A is from 0.8 to 1.0 and the others from 0.0 to 1.0. That is because the temperature range of binary mixture A is very small from 0.95 to 1.0.



Binary mixtures composing ternary mixture 1



Binary mixtures composing ternary mixture 2



Binary mixtures composing ternary mixture 3

Fig. 6.12 Critical curves (—) in p - T projection of the constituent binary mixtures which composed the ternary mixtures studied in this work. Critical points (○) of pure components are also illustrated.

The phase behaviour of ternary mixtures is studied and the results are showed in Fig 6.13 (mixture 1), 6.15 (mixture 2) and 6.18 (mixture 3). The Guggenheim equation of state is used for both binary and ternary calculations. The conformal parameters of three ternary mixtures are given in Table 6.5.

Table 6.5 Conformal parameters of ternary mixtures studied in detail *

| Ternary mixture | Sub binary mixtures | f_{11} | f_{22} | f_{33} | f_{12} | f_{13} | f_{23} |
|-----------------|---------------------|----------|----------|----------|----------|----------|----------|
| 1 | A, M, P | 1.0 | 0.95 | 0.485 | 0.975 | 0.696 | 0.679 |
| 2 | A, U, X | 1.0 | 0.95 | 0.43 | 0.975 | 0.656 | 0.639 |
| 3 | L, W, Y | 1.0 | 0.5 | 0.22 | 0.707 | 0.469 | 0.332 |

* The h conformal parameters are identical $h_{11} = h_{22} = h_{33} = h_{12} = h_{13} = h_{23} = 1$

Fig. 6.13 gives the isothermal-composition behaviour of the ternary mixture 1 at various temperatures. Binary mixture A is represented by mixture 1 + 2, binary mixture M is represented by mixture 1 + 3 and binary mixture P is represented by mixture 2 + 3. From Fig. 6.13, when $\tilde{p} = 0.9$, there are two critical curves, one is the liquid-liquid critical line (M_8, P_4) and another is liquid-vapour critical curve (M_7, P_3). When $p = 1.01$, the another side of liquid-vapour critical line (M_1, P_1) appears and then forms to a complete one curve (M_2, M_5 when $\tilde{p} = 1.1$). Eventually, at $\tilde{p} = 1.138$ the liquid-liquid (M_{11}, P_7) and liquid-vapour (M_3, M_4) curves meet together at point M_4 and M_{11} . The points M_1, M_2, \dots, M_{11} and P_1, P_2, \dots, P_7 in Fig 6.13 indicate the critical points of binary mixtures M and P.

For convenience, we present the critical properties of binary mixtures A, M and P in p - x projection (Fig. 6.14). In Fig. 6.14, the left hand side shows the whole picture for these three mixtures (binary mixture A, M and P) with the composition from 0 to 1 and the reduced pressure from 0 to 2. The right hand side of Fig. 6.14 shows a particular range of reduced pressure from 0.8 to 1.2 in which the critical properties of ternary mixture are examined. Comparing the points M_1, M_2, \dots, M_{11} and P_1, P_2, \dots, P_7 in Fig. 6.14 and Fig. 6.13 shows that they are identical .

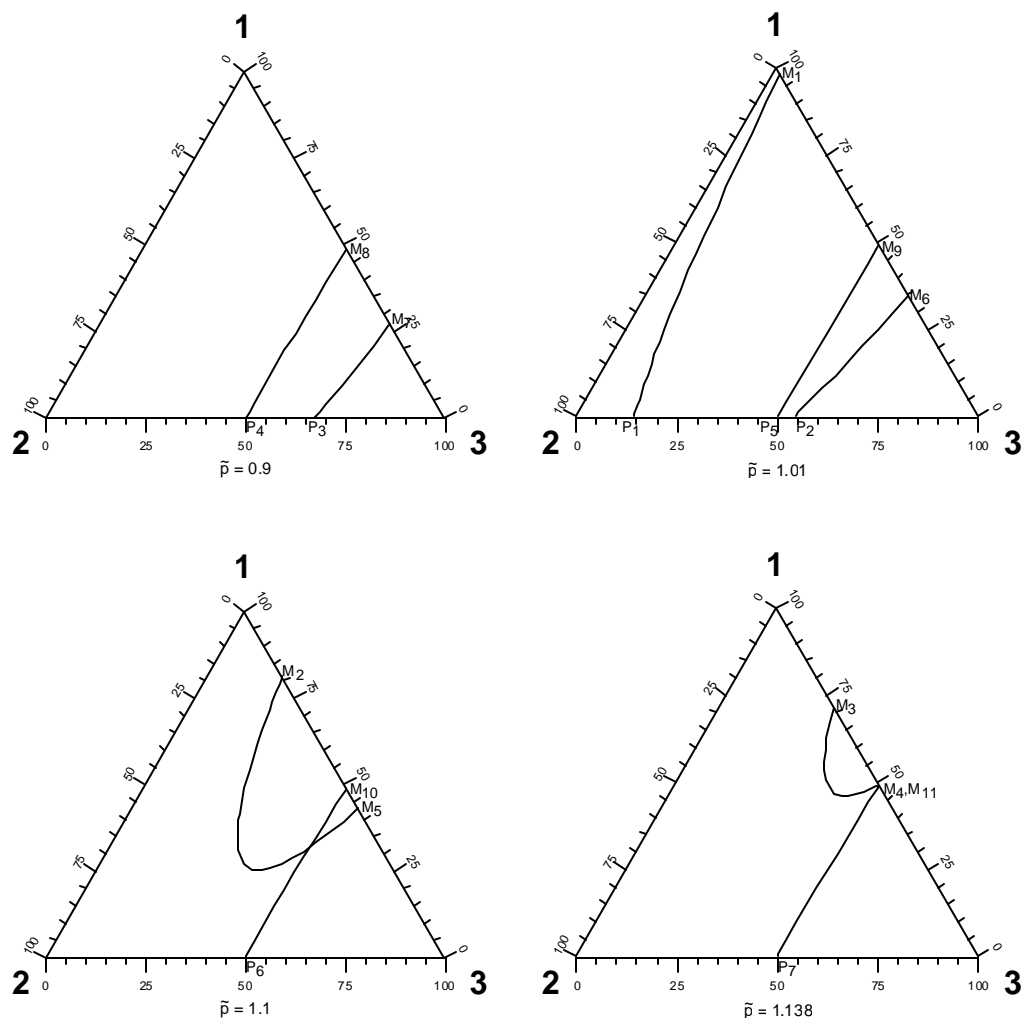


Fig. 6.13 The isothermal-composition critical behaviour of ternary mixture 1 (binary mixture A is mixture 1-2, binary mixture M is mixture 1-3, binary mixture P is mixture 2-3) at various temperatures. M_1, M_2, \dots, M_{11} and P_1, P_2, \dots, P_7 are the critical points of binary mixtures M and P.

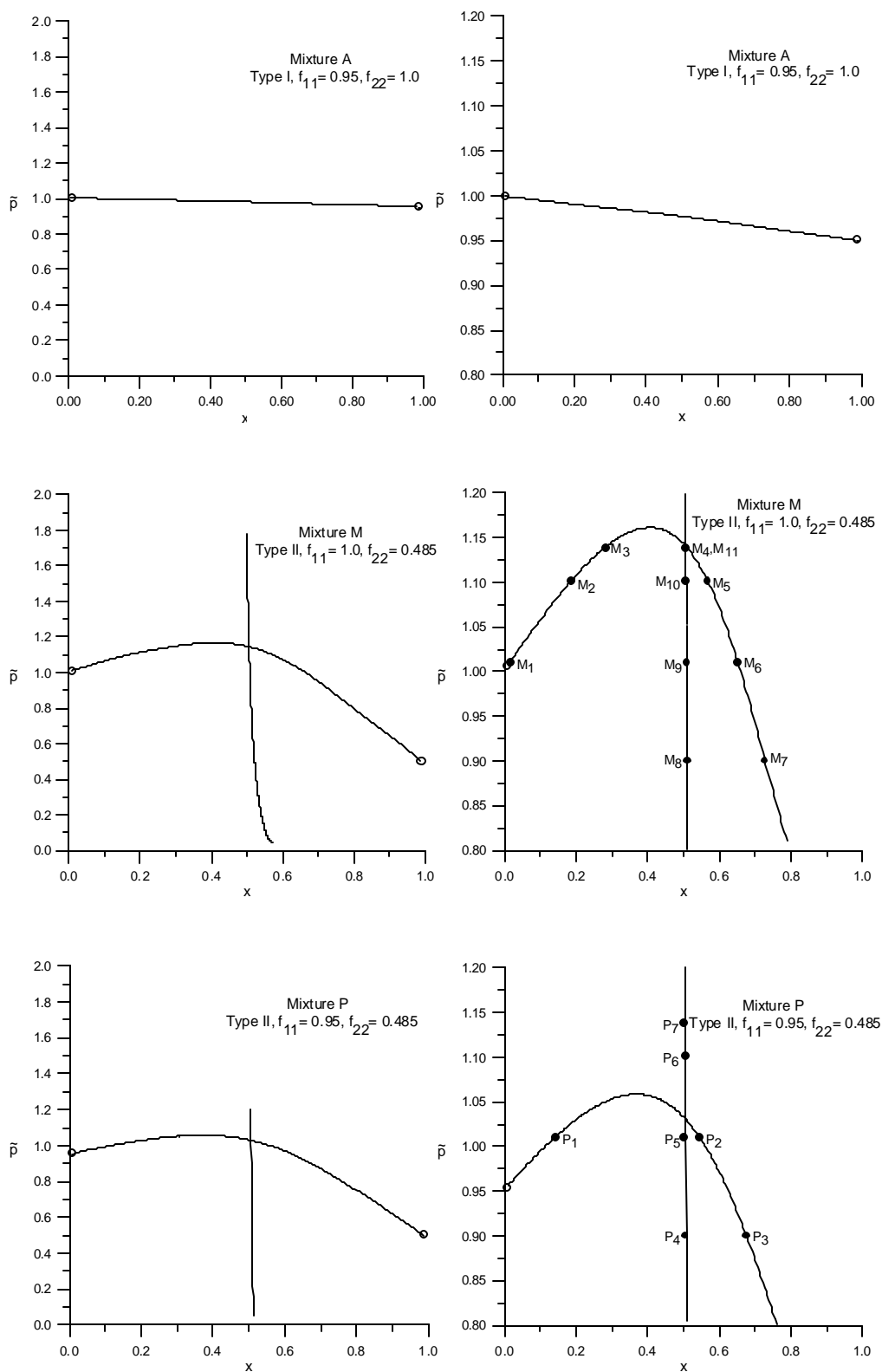


Fig. 6.14 Critical curves (—) of binary mixtures A, M, P in p - x projection. Critical points (○) of pure components and selected range (●) are also illustrated.

By using a similar idea, Fig. 6.15 gives the isothermal-composition behaviour of ternary mixture 2 at various temperatures. Binary mixture A is represented by mixture 1 + 2, binary mixture U is represented by mixture 1 + 3 and binary mixture X is represented by mixture 2 + 3. We choose 6 different pressures to look at the critical behaviour of ternary mixture 2. In Fig. 6.15, when $\tilde{p} = 1.0$, there is only one liquid-vapour critical curve. As the pressure is increased, the liquid-liquid critical line (U_1 , X_1) appears and the liquid-vapour critical line changes slightly. When $\tilde{p} = 1.19$, the liquid-liquid and liquid-vapour curves merge together, form one complete curve and show the continuity of vapour-liquid and liquid-liquid phenomena. Finally, at $\tilde{p} = 1.33$ the liquid-liquid and liquid-vapour curves meet together at a possible tricritical point. At $\tilde{p} = 1.4$, only liquid-liquid critical curve is left. In Fig. 6.16, the left hand side shows the whole picture of three binary mixtures (binary mixture A, U and X) with the composition from 0 to 1 and the reduced pressure from 0 to 2. The right hand side shows a particular range of reduced pressure from 0.8 to 1.5 in which the critical properties of ternary mixture are examined. So, comparing the U_1, U_2, \dots, U_5 and X_1, X_2, \dots, X_9 in Fig. 6.16 and Fig. 6.15 shows that they are identical. The binodal curves of this ternary mixture is also showed in Fig. 6.17 to highlight the continuity of vapour-liquid and liquid-liquid phenomena.

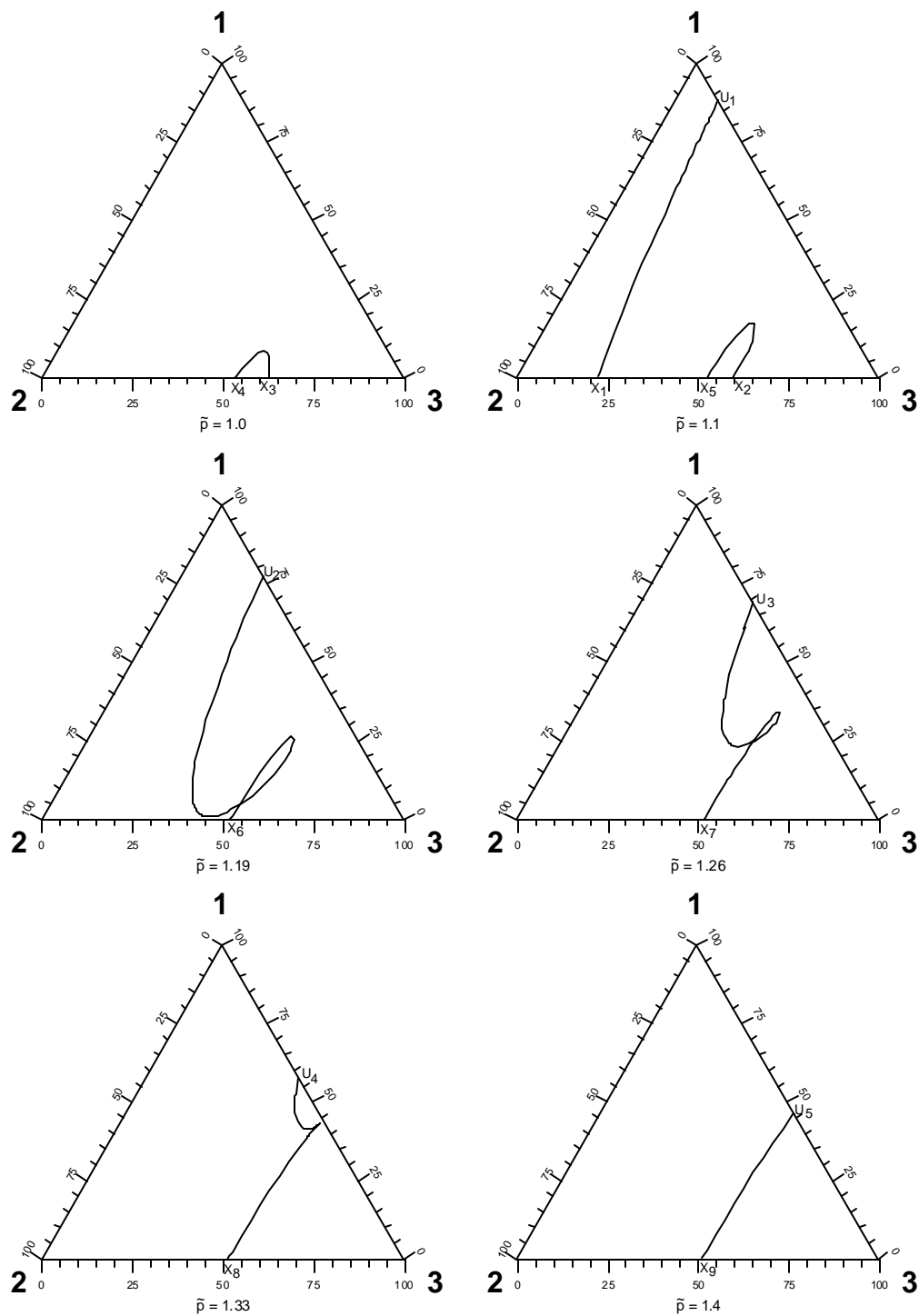


Fig. 6.15 The isothermal-composition critical behaviour of ternary mixture 2 (binary mixture A is mixture 1-2, binary mixture U is mixture 1-3, binary mixture X is mixture 2-3) at various temperatures. U_1, U_2, \dots, U_5 and X_1, X_2, \dots, X_9 are the critical points of binary mixtures U and X.

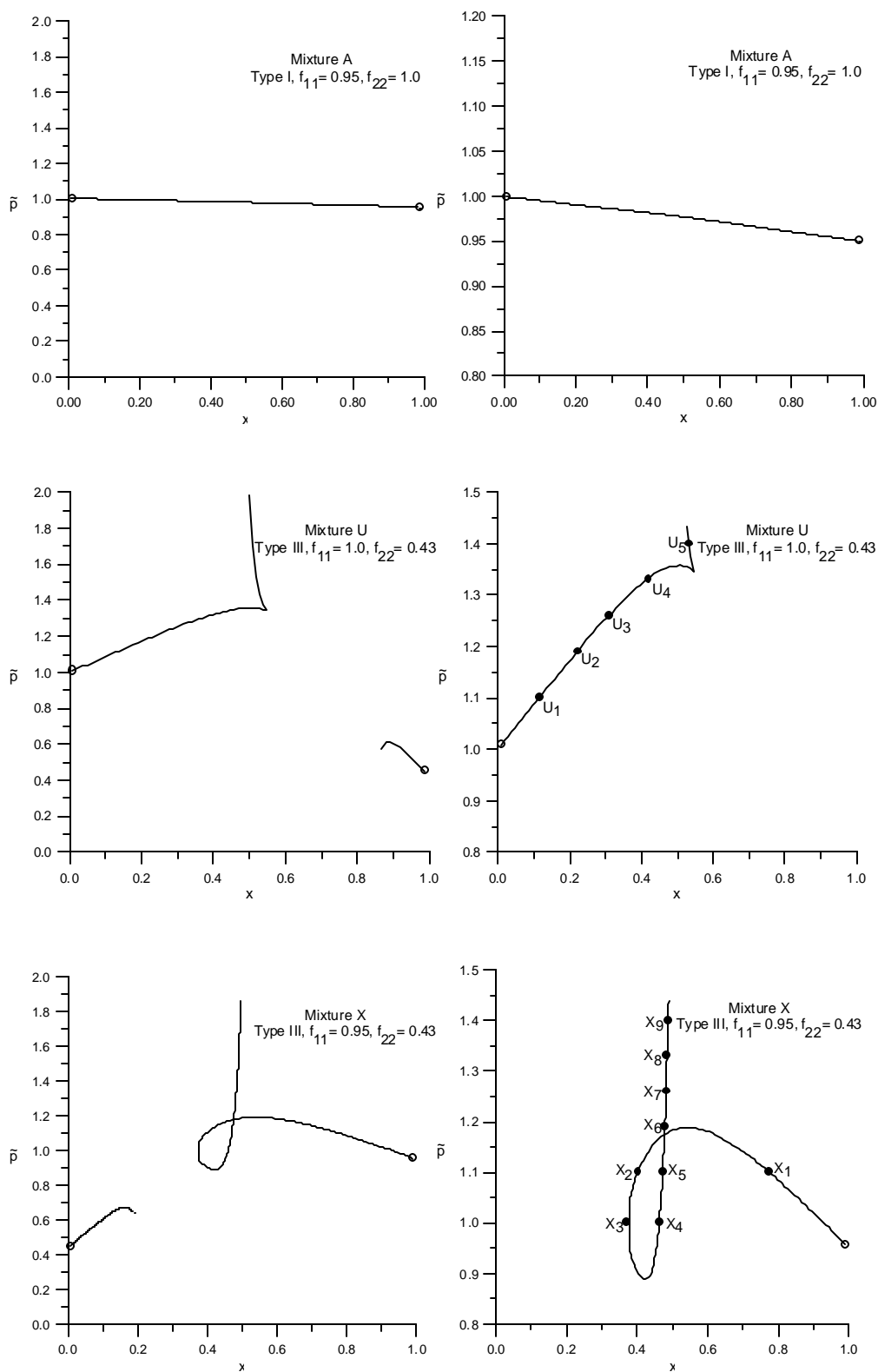


Fig. 6.16 Critical curves (—) of binary mixtures A, U, X in p - x projection. Critical points (O) of pure components and selected range (•) are also illustrated.

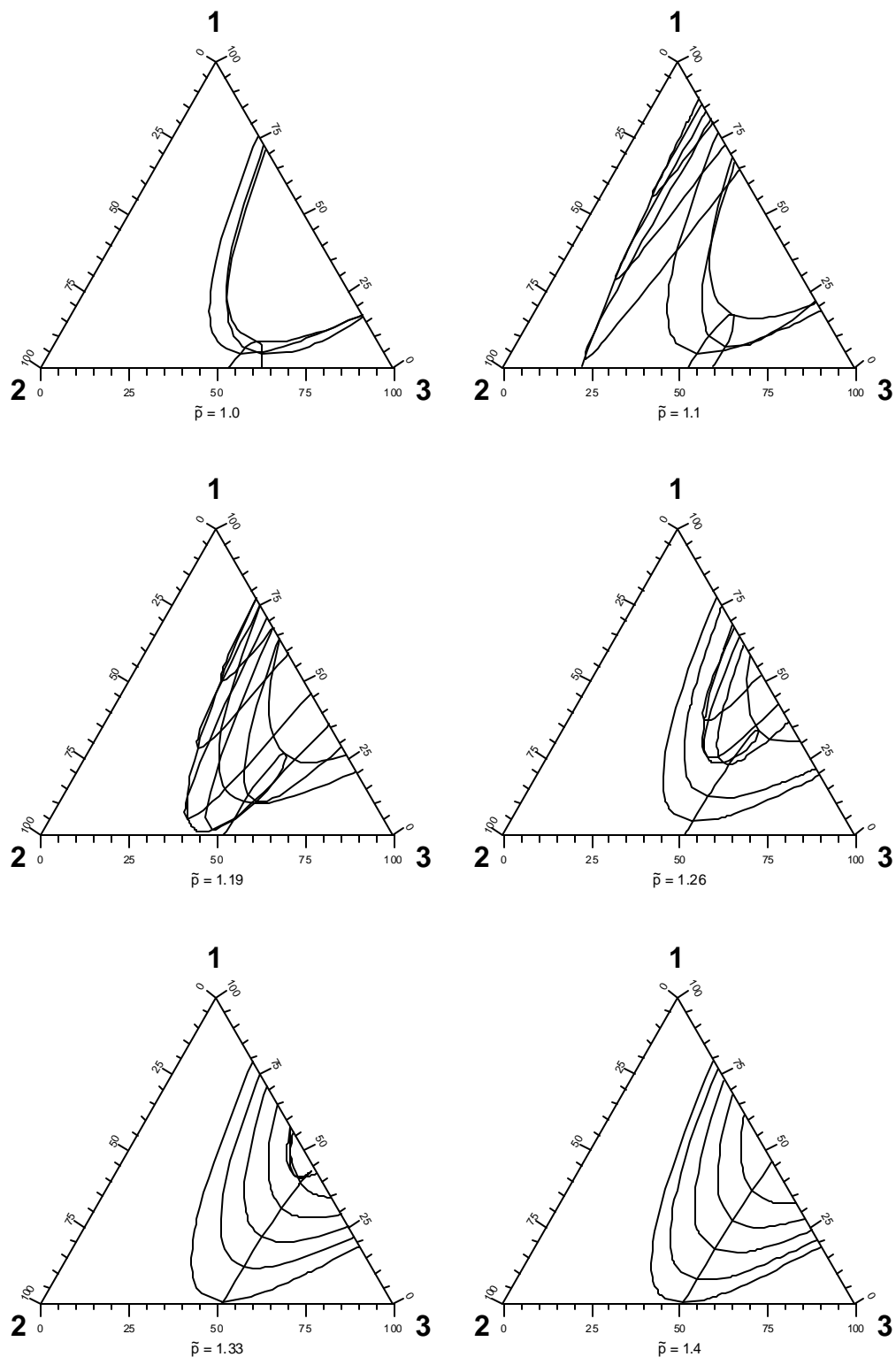


Fig. 6.17 The binodal (—) and critical equilibria ($\frac{3}{4}$) of ternary mixture 2 (binary mixture A is mixture 1-2, binary mixture U is mixture 1-3, binary mixture X is mixture 2-3) at various temperatures.

Fig. 6.18 gives the isothermal-composition behaviour of ternary mixture 3 at various temperatures. Binary mixture L is represented by mixture 1 + 2, binary mixture W is represented by mixture 1 + 3 and binary mixture Y is represented by mixture 2 + 3. In Fig. 6.18, when $\tilde{p} = 0.9$, the curve started from L_1 exhibits the vapour-liquid (curve VL1) behaviour and the curve started from L_2 exhibits the liquid-liquid behaviour. These two curves meet at a possible tricritical point. This shows continuity between vapour-liquid and liquid-liquid equilibria. Another curve started from Y_1 is vapour-liquid (curve VL2) critical curve which is not completed because the limitation of calculation. As the pressure is increased, the curve VL2 changes slightly, but the end of critical point of liquid-liquid critical line goes to binary mixture W. When $\tilde{p} = 1.5$ and $\tilde{p} = 2.0$, the VL1 and liquid-liquid curves connect smoothly and show a continuous vapour-liquid and liquid-liquid transition. In Fig. 6.19, the left hand side shows the whole picture of these three mixtures (binary mixture L, W and Y) with the composition from 0 to 1 and the reduced pressure from 0 to 2. The right hand side shows a particular range of reduced pressure from 0.8 to 2.0 in which the critical properties of ternary mixture 3 are examined. So, comparing the points, $L_1, L_2, \dots, L_5, W_1, W_2, W_3$ and Y_1, Y_2, \dots, Y_4 in Fig. 6.18 and Fig. 6.19 shows that they are identical.

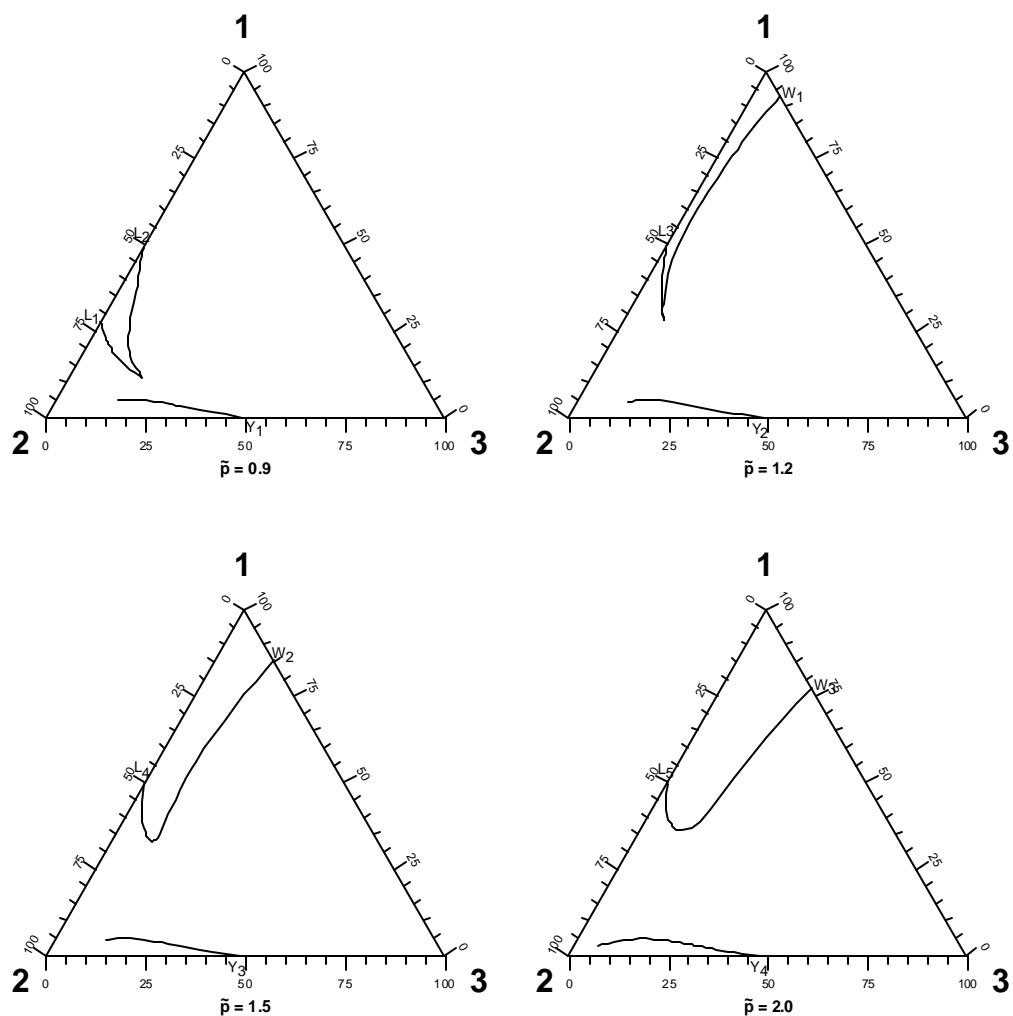


Fig. 6.18 The isothermal-composition critical behaviour of ternary mixture 3 (binary mixture L is mixture 1-2, binary mixture W is mixture 1-3, binary mixture Y is mixture 2-3) at various temperatures. $L_1, L_2, \dots, L_5, W_1, W_2, W_3$ and Y_1, Y_2, \dots, Y_4 are the critical points of binary mixtures L, W, Y.

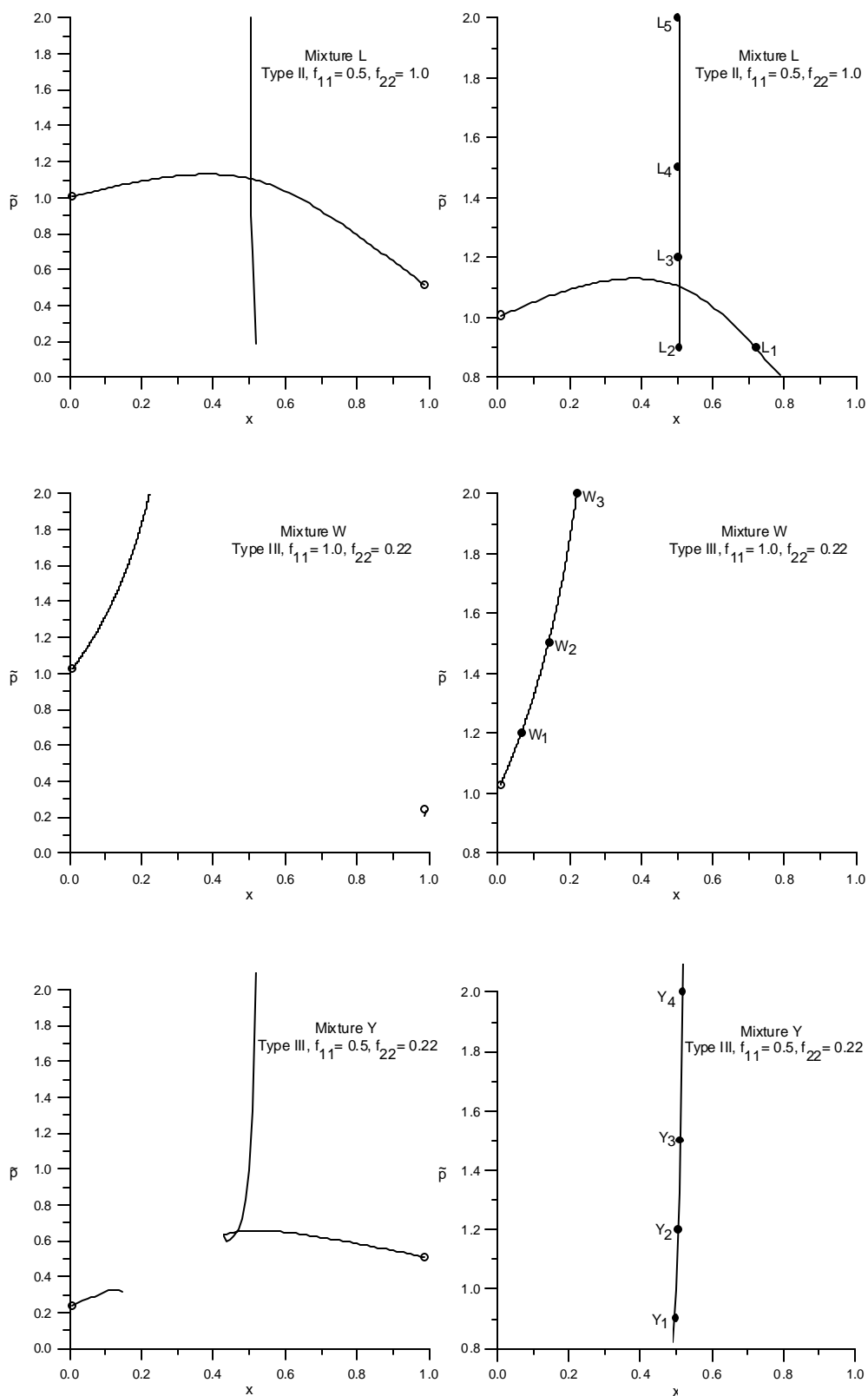


Fig. 6.19 Critical curves (—) of binary mixtures L, W, Y in p - x projection. Critical points (○) of pure components and selected range (●) are also illustrated.

References

- Brandt, E. (1987) Experimentelle Bestimmung von Phasengleichgewichten ternärer, fluider, wasserhaltiger Systeme bis zu hohen Drücken und Temperaturen. Dr.-Ing., Universität Karlsruhe, Germany.
- Brunner, E. (1988). Fluid Mixtures at High Pressures VII. Phase Separations and Critical Phenomena in 12 Binary Mixtures Containing Ammonia. *J. Chem. Thermodynamics*, **20**, 1379-1409.
- Brunner, E. (1990). Fluid Mixtures at High Pressures: IX. Phase Separation and Critical Phenomena in 23 (n-Alkane + Water) Mixtures. *J. Chem. Thermodynamics*, **22**, 335-353.
- Guggenheim, E. A. (1965). Variations on van der Waals' Equation of State for High Densities. *Mol. Phys.*, **9**, 199-200.
- Heilig, M. and Franck, E.U. (1989). Calculation of Thermodynamic Properties of Binary Fluid Mixtures to High Temperatures and Pressures. *Ber. Bunsenges. Phys. Chem.*, **93**, 898-905.
- Hicks, C. P. and Young, C. L. (1975). The Gas-Liquid Critical Properties of Binary Mixtures. *Chem. Rev.*, **75**, 119-175.
- Kay, W. B. and Kreglewski, A. (1983) Critical-Locus Curves and Liquid-Vapour Equilibria in the Binary Systems of Benzene with Carbon Dioxide and Sulfur Dioxide. *Fluid Phase Equilib.*, **11**, 251-265.
- McGlashan, M. L. (1985). Phase Equilibria in Fluid Mixtures. *Pure Appl. Chem.*, **57**, 89-103.
- Rowlinson, J. S., Sutton, J. R. and Weston, F. (1958). Liquid-Vapour Equilibrium in the Ternary System Carbon Dioxide - Nitrous Oxide - Ethylene. *Proc. Conf. Thermodynamic and Transport Properties Fluids*. 10-14.
- Rowlinson, J. S. and Swinton, F. L. (1982). *Liquids and Liquid Mixtures*, 3rd Ed., Butterworths, London.
- Sadus, R.J. (1992a). *High Pressure Phase Behaviour of Multicomponent Fluid Mixtures*, Elsevier, Amsterdam.
- Sadus, R. J. (1992b). Novel Critical Transitions in Ternary Fluid Mixtures. *J. Phys. Chem.*, **96**, 5197-5202.
- Sadus, R. J. (1993). Novel High Pressure Phase Transitions of Multicomponent Fluid Mixtures. *Fluid Phase Equilibria*, **83**, 101-108.

- Sadus, R. J. (1994). Calculating Critical Transitions of Fluid Mixtures: Theory vs. Experiment. *AIChE J.*, **40**, 1376-1403.
- Schneider, G.M. (1978). In McGlashan, M.L. (Ed.), *Chemical Thermodynamics Vol. 2, A Specialist Periodical Report*, The Chemical Society, London.
- Temkin, M. I. (1969). Conditions Governing the Coexistence of Gaseous Phases. *Russ. J. Phys. Chem.*, **33**, 275-277.
- Tödheide, K. and Franck, E. U. (1963) Das Zweiphasengebiet und die kritische Kurve im System Kohlendioxid – Wasser bis zu Drucken von 3500 bar. *Z. f. Physik. Chem.*, **37**, 387-401.
- Tsiklis, D. S. (1952). Limited Mutual solubility in the Gas Systems Ammonia - Helium and Helium - Carbon Dioxide under High Pressure. *Doklady Akad. Nauk SSSR*, **86**, 1159-1161.
- Tsiklis, D. S. (1953). Limited Mutual solubility in the Gas System Helium - Ethylene under High Pressure. *Doklady Akad. Nauk SSSR*, **91**, 1361-1363.
- Tsiklis, D. S., Maslennikova, V. Ya. and Orlova, A. A. (1970). Mutual Finite Solubility of Gases in the Three-Component System Helium-Ethylene-Carbon Dioxide. *Doklady Akad. Nauk SSSR*, **195**, 1381-1384. [*Doklady Phys. Chem.*, **195**, 994-997]
- Van Konynenburg, P. H. and Scott, R. L. (1980). Critical Lines and Phase Equilibria in Binary van der Waals Mixtures. *Philos. Trans. Roy. Soc. London A*, **298**, 495-540.